Article

Not peer-reviewed version

New Progress on London Dispersive Energy, Polar Surface Interactions and Lewis's Acid-Base Properties of Solid Surfaces

Tayssir Hamieh *

Posted Date: 8 January 2024

doi: 10.20944/preprints202401.0638.v1

Keywords: London dispersive energy; polar energy of adsorption; polar enthalpy and entropy of adsorption; enthalpic and entropic Lewis's acid base parameters; separation distance between particles; acid-base surface energy.

Article

New Progress on London Dispersive Energy, Polar Surface Interactions and Lewis's Acid-Base Properties of Solid Surfaces

Tayssir Hamieh [1,2]

[1] Faculty of Science and Engineering, Maastricht University, P.O. Box 616, 6200 MD Maastricht, The Netherlands, Email: t.hamieh@maastrichtuniversity.nl, Tel.: +31 6 5723 9324.
[2] Laboratory of Materials, Catalysis, Environment and Analytical Methods Laboratory (MCEMA), Faculty of Sciences, Lebanese University, Hadath, Lebanon

Abstract: The determination of the specific surface free energy, specific properties and Lewis's acid base of solid materials is of capital importance in many industrial processes such as adhesion, coatings, two dimensional films and adsorption phenomena. (1) Background: The physicochemical properties of many solid particles were characterized during the last forty years by using the retention time of injected well-known molecules into chromatographic column containing the solid substrates to be characterized. The obtained net retention time of the solvents adsorbed on the solid allowing the determination of the net retention volume directly correlated to the specific surface variables, dispersive, polar and acid-base properties. (2) Methods: Many chromatographic methods were used to quantify the values of the different specific surface variables of the solids. However, one found a large deviation between the different results. In this paper, one proposed a new method that quantify the specific free energy of adsorption as well as the Lewis's acid-base constants of many solid surfaces. (3) Results: The new applied method allowed us to obtain the specific enthalpy and entropy of adsorption of polar model organic molecules on several solid substrates such as silica, alumina, MgO, ZnO, Zn, TiO_2 and carbon fibers. (4) Conclusions: our new method based on the separation between the dispersive and polar free surface energy allowed to better characterize the solid materials.

Keywords: London dispersive energy; polar energy of adsorption; polar enthalpy and entropy of adsorption; enthalpic and entropic Lewis's acid base parameters; separation distance between particles; acid-base surface energy.

1. Introduction

Dispersion and polar interactions are the two important types of interactions between particles. The determination of these interactions is very used in the different domains of colloidal science, surface physics, adsorption, adhesion, adsorption, surface and interface. The dispersive interactions were studied and well-developed by Van der Waals. The corresponding forces, called Van der Waals forces, results from the temporary fluctuations in the charge distribution of the atoms or molecules; whereas, the polar forces or interactions include Coulomb interactions between permanent dipoles and between permanent and induced dipoles. The total interaction energy is the sum of the dispersive and polar interaction energies. The separation of these two types of energy is crucial to understand the behavior of molecules and therefore to predict the various surface physicochemical properties of materials and nanomaterials.

Since 1982, many scientists proposed several methods to separate the dispersive (or London) and polar (or specific) interactions between a solid substrate and a polar molecule. The first attempt for the separation of the two above contributions was proposed by Saint-Flour and Papirer [1-3] when studying untreated and silane-treated glass fibers by using inverse gas chromatography (IGC) and choosing a series of polar and non-polar adsorbates to quantify the dispersive and polar free energies. The authors adopted the concept of the vapor pressure P_0 of the adsorbates to determine the specific

Preprints (www.preprints.org) | NOT PEER-REVIEWED | Posted: 8 January 2024 doi:10.20944/preprints202401.0638.v1

free energy of adsorption $\Delta G_a^{sp}(T)$ of polar molecules on glass fibers as a function of the absolute temperature T by plotting the variations of $RTlnVn$ versus the logarithm of the vapor pressure P_0 of probe, where Vn is the net retention volume and R the ideal gas constant. Saint-Flour and Papirer [3] determined the specific enthalpy ΔH_a^{sp} and entropy ΔS_a^{sp} of polar molecules adsorbed on the glass fibers and deduced their Lewis acid-base constants. Later, Schultz et al. [4] tried to separate the two dispersive and specific interactions of carbon fibers by using the concept of the dispersive component γ_l^d of the surface energy of the organic liquids by drawing $RTlnVn$ of as a function of $2\mathcal{N}a\sqrt{\gamma_l^d}$ of n-alkanes and polar molecules adsorbed on the solid, where a is the surface area of adsorbed molecule and $\mathcal{N}$ the Avogadro's number. This method allowed to obtain the specific free energy and the dispersive component γ_s^d of the surface energy of carbon fibers. In 1991, Donnet et al. [5]. used the deformation polarizability $\alpha_{0,L}$ of solvents and obtained the specific free energy $\Delta G_a^{sp}(T)$ of polar solvents adsorbed on natural graphite powders by representing the variations of as a function of $\sqrt{h\nu_L}\,\alpha_{0,L}$, where ν_L is the electronic frequency of the probe and h the Planck's constant. With the difficulties and issues encountered with the previous methods, Brendlé and Papirer [6,7] used the topological index χ_T, derived from the well-known Wiener index to obtain more accurate results. Other methods were also used in literature such as that the boiling point $T_{B.P.}$ [8] and the standard enthalpy of vaporization $\Delta H_{vap.}^0$ [9]. In all the above methods, one obtained an excellent linearity of $RTlnVn$ of n-alkanes as a function of the chosen intrinsic thermodynamic parameter (lnP_0, $a\sqrt{\gamma_l^d}$, $\sqrt{h\nu_L}\,\alpha_{0,L}$, $T_{B.P.}$ or $\Delta H_{vap.}^0$). The specific free potential $\Delta G_a^{sp}(T)$ of polar molecule is then directly obtained by the distance the point representing the polar molecule to its hypothetic point located on the n-alkane straight-line. The specific enthalpy and entropy of adsorbed polar solvents as well as the Lewis acid base constants can easily deduced by thermodynamic considerations. The serious problem encountered in these different chromatographic methods that the obtained

One proved in several previous studies the non-validity of the method used by Schultz et al. due to the variations of the surface area a and γ_l^d of solvents as a function of the temperature [10-14]. The values of the surface area of organic molecules versus the temperature obtained on a certain solid material [10-14], cannot be always transferred to another solid, because of the different behaviors existing between the various solid surfaces and the adsorbed molecules.

The used chromatographic methods, even if they satisfied linear relations for n-alkanes adsorbed on solid surfaces, cannot be necessarily considered as accurate if they are not theoretically well-founded. One proved in previous paper [11,12] that the linearity of $RTlnVn$ of n-alkanes is satisfied for more than twenty intrinsic thermodynamic parameters and one concluded on the necessity to find new methods that are theoretically valid.

Given the disparity of the results obtained from the application of the various methods, one privileged, in this paper, the method based on the equation of the London dispersive interaction [15] between the solvents and the solid materials. By using the London equation (15), one proposed in this study to determine the dispersive free energy ΔG_a^d, the specific free energy ΔG_a^{sp}, the Lewis acid-base constants and the polar acidic and basic surface energy of several solid materials such as silica (SiO_2), alumina (Al_2O_3), magnesium oxide (MgO), zinc oxide (ZnO), Monogal-Zn, titanium dioxide (TiO_2) and carbon fibers.

2. Methods and models

Inverse gas chromatography (IGC) technique [16-24] was used in this study to characterize the surface properties of the above solid surfaces. IGC allowed us to obtain the net retention time and therefore the net retention volume of the various solvents adsorbed on the different solid materials. This allowed to obtain the free energy of adsorption ΔG_a^0 of the adsorbed molecules by using the following fundamental equation of IGC:

$$\Delta G_a^0(T) = -RTlnVn + C(T) \qquad (1)$$

Preprints (www.preprints.org) | NOT PEER-REVIEWED | Posted: 8 January 2024 doi:10.20944/preprints202401.0638.v1

where $C(T)$ is a constant depending on the temperature and the parameters of interaction between the solid and the solvent.

The total free energy of adsorption $\Delta G_a^0(T)$ is composed by the two dispersive $\Delta G_a^d(T)$ and polar $\Delta G_a^{sp}(T)$ contributions of the total interaction energy:

$$\Delta G_a^0(T) = \Delta G_a^d(T) + \Delta G_a^{sp}(T) \quad (2)$$

The free dispersive energy between two non-identical materials was given by London [15]:

$$-\Delta G_a^d(T) = \frac{3}{2}\frac{\alpha_{01}\,\alpha_{02}}{(4\pi\varepsilon_0)^2\,H^6}\frac{R\,\nu_1\,\nu_2}{(\nu_1+\,\nu_2)} = \frac{3}{2}\frac{\alpha_{01}\,\alpha_{02}}{(4\pi\varepsilon_0)^2\,H^6}\frac{\mathcal{N}\,\varepsilon_1\,\varepsilon_2}{(\varepsilon_1+\,\varepsilon_2)} \quad (3)$$

where α_{01} and α_{02} are the respective deformation polarizabilities of molecules 1 and 2 separated by a distance H, ε_1 and ε_2 the ionization energies of molecules 1 and 2, ν_1 and ν_2 their characteristic electronic frequencies and ε_0 the permittivity of vacuum.

By denoting S the solid molecule 1 and X the probe molecule 2 and combining the previous equations (1-3), one obtained equation (4):

$$\Delta G_a^0(T) = -RTlnVn + C(T) = -\frac{\alpha_{0S}}{H^6}\left[\frac{3\mathcal{N}}{2(4\pi\varepsilon_0)^2}\left(\frac{\varepsilon_S\,\varepsilon_X}{(\varepsilon_S+\,\varepsilon_X)}\alpha_{0X}\right)\right] + \Delta G_a^{sp}(T) \quad (4)$$

The thermodynamic parameter $\mathcal{P}_{SX}$ chosen as new indicator variable in this original contribution is given by relation (5):

$$\mathcal{P}_{SX} = \frac{\varepsilon_S\,\varepsilon_X}{(\varepsilon_S+\,\varepsilon_X)}\alpha_{0X} \quad (5)$$

Indeed, the London dispersion interactions strongly depend on the deformation polarizability of the organic molecules and on the ionization energies of the solid and the solvents, because the approximation $\frac{\varepsilon_S\,\varepsilon_X}{(\varepsilon_S+\,\varepsilon_X)} \approx \frac{\sqrt{\varepsilon_S\,\varepsilon_X}}{2}$ is not always valid and it depends on the product of the ionization energies $\varepsilon_S\,\varepsilon_X$. To avoid any source of errors on the determination of the London dispersive and polar energies, one privileged to use the true values of the ionization energies and not the approximation of the geometric mean.

Now, by drawing the variations of $RTlnVn$ of n-alkanes adsorbed on the solid material as a function of $\left[\frac{3\mathcal{N}}{2(4\pi\varepsilon_0)^2}\left(\frac{\varepsilon_S\,\varepsilon_X}{(\varepsilon_S+\,\varepsilon_X)}\alpha_{0X}\right)\right]$ at a fixed temperature T, one obtained the linear equation given by (6):

$$RTlnVn(n-alkane) = A\left[\frac{3\mathcal{N}}{2(4\pi\varepsilon_0)^2}\mathcal{P}_{SX(n-alkane)}\right] - C \quad (6)$$

where A is the slope of the n-alkanes straight line given by (7):

$$A = \frac{\alpha_{0S}}{H^6} \quad (7)$$

In the case of adsorbed polar organic molecule such as toulene, the distance between its representative point given by $RTlnVn(Toluene)$ and the straight-line of n-alkanes shown on Figure 1, allowed to obtain the polar free energy $\Delta G_a^{sp}(Toluene)$ (London dispersion interaction).

Preprints (www.preprints.org) | NOT PEER-REVIEWED | Posted: 8 January 2024 doi:10.20944/preprints202401.0638.v1

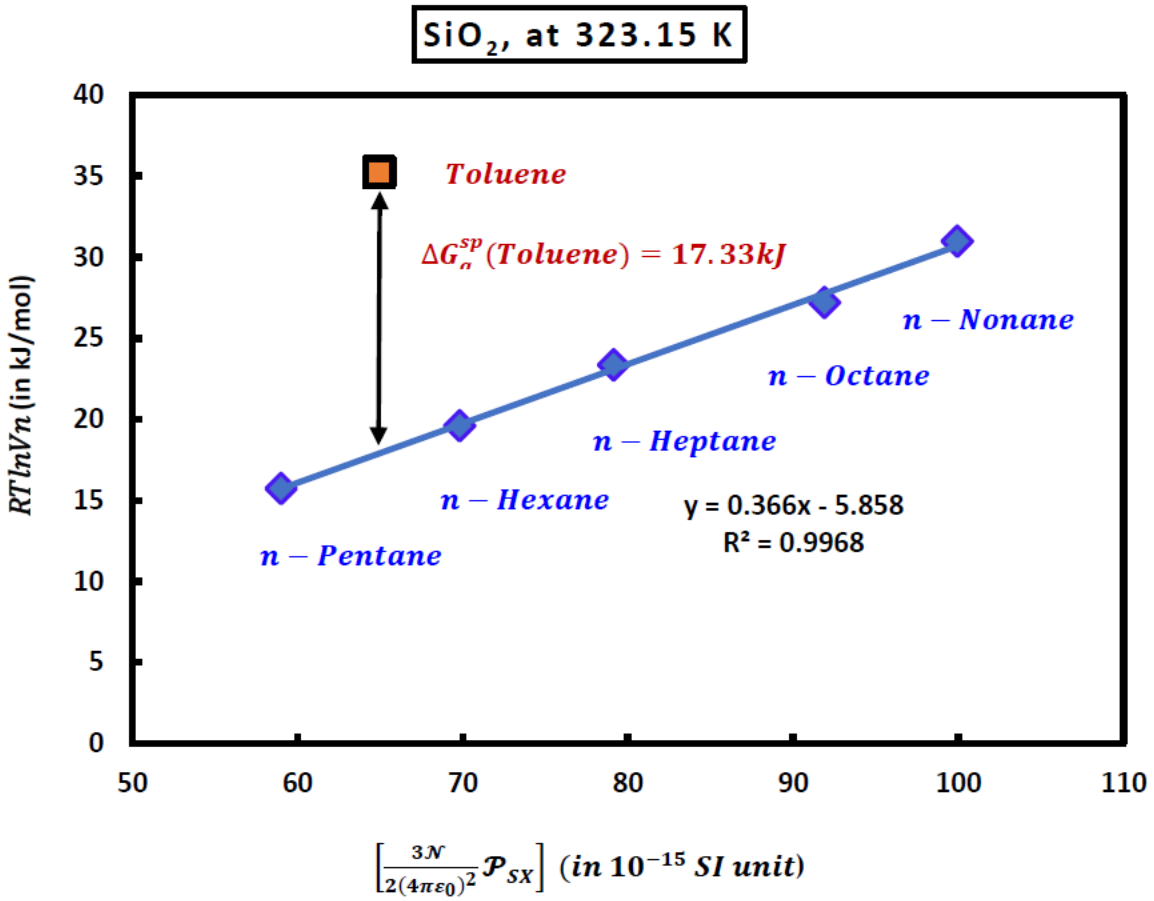

Figure 1. Variations of $RTlnVn$ of n-alkanes and toluene adsorbed on the silica particles as a function of $\left[\frac{3\mathcal{N}}{2(4\pi\varepsilon_0)^2}\mathcal{P}_{SX}\right]$ at *T*=323.15K.

The numerical value of the London dispersion interaction of toluene (in kJ/mol) adsorbed on silica particles is given by the following equation

$$\Delta G_a^{sp} = RTlnVn - [0.366(in\ kJ/(10^{-15}SI)] \times \frac{3\mathcal{N}}{2(4\pi\varepsilon_0)^2}\mathcal{P}_{SiO_2-Toluene}(in10^{-15}SI) \qquad (8)$$

Experimental results gave at 323.15K:

$$RTlnVn(Toluene) = 35.225\ kJ/mol\ ;\ \frac{3\mathcal{N}}{2(4\pi\varepsilon_0)^2}\mathcal{P}_{SiO_2-Toluene} = 64.954 \times 10^{-15} SI\ uni \qquad (9)$$

And one obtained at this temperature the value of the specific free energy of toluene from (8):

$$\Delta G_a^{sp}(Toluene) = 17.330\ kJ/mol \qquad (10)$$

By varying the temperature, the calculations allowed to determine the variations of $\Delta G_a^{sp}(T)$ of polar probes as a function of the temperature and obtain the specific enthalpy $\left(-\Delta H_a^{sp}\right)$ and entropy $\left(\Delta S_a^{sp}\right)$ of the various polar probes adsorbed on the solid surfaces from equation (11):

$$\Delta G_a^{sp}(T) = \Delta H_a^{sp} - T\,\Delta S_a^{sp} \qquad (11)$$

And then to deduce the Lewis's acid base constants K_A and K_D by equation (12):

$$-\Delta H^{Sp} = K_A \times DN + K_D \times AN \qquad (12)$$

where *AN* and *DN* are respectively the electron donor and acceptor numbers of the polar molecule. These numbers were calculated by Gutmann [25] and corrected by Fowkes [26].

Preprints (www.preprints.org) | NOT PEER-REVIEWED | Posted: 8 January 2024 doi:10.20944/preprints202401.0638.v1

By using the representation $\frac{-\Delta H^{Sp}}{AN} = f\left(\frac{DN}{AN}\right)$ and equation (13):

$$-\frac{\Delta H^{Sp}}{AN} = K_A \frac{DN}{AN} + K_D \tag{13}$$

The slope of the straight-line gave the acidic constant K_A, whereas, the basic constant K_D is obtained by the ordinate at origin of the straight-line given by equation (13).

However, in many cases, one proved that equation (13) is not verified and one previously proposed another relation taking into account the amphoteric effect of the solid material [27].

$$-\Delta H^{Sp} = K_A \times DN + K_D \times AN - K_{CC} \times AN \times DN \tag{14}$$

where K_{CC} is the coupling constant representing the amphoteric character of material.

Equation (14) can be written as:

$$-\frac{\Delta H^{Sp}}{AN} = K_A \frac{DN}{AN} + K_D - K_{CC} \times DN \tag{15}$$

By considering a polar molecule symbolized by (i) and putting:

$$\begin{cases} (x_1)_i = -\frac{\Delta H^{Sp}}{AN} \\ (x_2)_i = \frac{DN}{AN} \\ (x_3)_i = K_D \end{cases} \tag{16}$$

One can write the general equation (17) representing any polar molecule (i) in interaction with solid surfaces:

$$(x_1)_i = K_D + K_A (x_2)_i - K_{CC} \times (x_3)_i \tag{17}$$

where $(x_1)_i$, $(x_2)_i$ and $(x_2)_i$ are experimentally well-known, whereas, K_D, K_A and K_{CC} are the unkown quantities of the problem (17).

For n polar molecules ($n \geq 3$), the solution of the linear system (17) can be obtained by the least squares method by finding the vector $(K_D; K_A; -K_{CC})$ that minimizes the sum of the squares of the residuals.

In this case, The system of equations (17) will be transformed to a linear system represented by the following equations:

$$\begin{cases} \sum_{i=1}^{n} (x_1)_i = K_D n + K_A \sum_{i=1}^{n} (x_2)_i - K_{CC} \sum_{i=1}^{n} (x_3)_i \\ \sum_{i=1}^{n} [(x_1)_i (x_2)_i] = K_D \sum_{i=1}^{n} (x_2)_i + K_A \sum_{i=1}^{n} [(x_2)_i]^2 - K_{CC} \sum_{i=1}^{n} [(x_2)_i (x_3)_i] \\ \sum_{i=1}^{n} [(x_1)_i (x_3)_i] = K_D \sum_{i=1}^{n} (x_3)_i + K_A \sum_{i=1}^{n} [(x_2)_i (x_3)_i] - K_{CC} \sum_{i=1}^{n} [(x_3)_i]^2 \end{cases} \tag{18}$$

Equations (18) can be represented by the following matrix system

Preprints (www.preprints.org) | NOT PEER-REVIEWED | Posted: 8 January 2024 doi:10.20944/preprints202401.0638.v1

$$\begin{pmatrix} n & \sum_{i=1}^{n}(x_2)_i & \sum_{i=1}^{n}(x_3)_i \\ \sum_{i=1}^{n}(x_2)_i & \sum_{i=1}^{n}[(x_2)_i]^2 & \sum_{i=1}^{n}[(x_2)_i(x_3)_i] \\ \sum_{i=1}^{n}(x_3)_i & \sum_{i=1}^{n}[(x_2)_i(x_3)_i] & \sum_{i=1}^{n}[(x_3)_i]^2 \end{pmatrix} \times \begin{pmatrix} K_D \\ K_A \\ -K_{CC} \end{pmatrix} = \begin{pmatrix} \sum_{i=1}^{n}(x_1)_i \\ \sum_{i=1}^{n}[(x_1)_i(x_2)_i] \\ \sum_{i=1}^{n}[(x_1)_i(x_3)_i] \end{pmatrix} \quad (19)$$

Symbolized by the matrix equation:

$$AX = B \quad (20)$$

The matrix equation is inversible because the matrix A is symmetric and then there is a unique solution $X = (K_D;\ K_A; -K_{CC})$ given by the formal equation (21):

$$X = A^{-1} \times B \quad (21)$$

Our method was used in all solid materials that did not satisfy the classic equation (13).

In this study, one also determined the Lewis entropic acidic ω_A and basic ω_D parameters to obtain the Lewis entropic acid base character of the solid materials. The equations (22) and (23) were given by analogy that of the Lewis enthalpic acid-base constants K_A and K_D:

$$\left(-\Delta S_a^{sp}\right) = \omega_A\, DN' + \omega_D\, AN' \quad (22)$$

or

$$\left(\frac{-\Delta S_a^{sp}}{AN'}\right) = \omega_A \left(\frac{DN'}{AN'}\right) + \omega_D \quad (23)$$

3. Materials and solvents

One used in this paper several solid materials such as silica (SiO_2), alumina (Al_2O_3), magnesium oxide (MgO), zinc oxide (ZnO), Monogal-Zn, titanium dioxide (TiO_2) and carbon fibers that were characterized in previous papers [10-14] with other chromatographic methods and molecular models. The organic solvents such as n-alkanes and polar molecules were those previously used in other studies. The donor and acceptor numbers of electron used in this paper were those calculated and corrected by by Riddle and Fowkes [26]. The chromatographic measurements were obtained from a Focus GC Chromatograph equipped with a flame ionization detector of high sensitivity. All experimental methods on this technique were previously explained in details in previous papers [10-14].

4. Results

4.1. New approach for the calculation of the deformation polarizability α_{0X} and the indicator parameter $\mathcal{P}_{SX}$

Our new approach previously presented allowed us to obtain all necessary parameters of organic solvents and solid substrates by using their values taken from the Handbook of Physics and Chemistry [28]. The obtained results are presented below on Tables 1–8.

The new values of the various parameters given in Tables 1–8 were used in our new method to give the new values of London dispersive and polar energies of the various solid materials.

Table 1. Values of deformation polarizability (in 10^{-30} m^3) and (in 10^{-40} C m^2/V) and ionization energy (in eV) of the various organic molecules and solid materials.

Molecule	ε_X or ε_X	α_{0X} or α_{0S}	α_{0X} or α_{0S}

Preprints (www.preprints.org) | NOT PEER-REVIEWED | Posted: 8 January 2024 doi:10.20944/preprints202401.0638.v1

	(eV)	(in 10^{-30} m^3)	(in 10^{-40} C m^2/V)
n-pentane	10.28	9.99	11.12
n-hexane	10.13	11.90	13.24
n-heptane	9.93	13.61	15.14
n-octane	9.80	15.90	17.69
n-nonane	9.71	17.36	19.32
n-decane	9.65	19.10	21.25
CCl_4	11.47	10.85	12.07
Nitromethane	11.08	7.37	8.20
CH_2Cl_2	11.32	7.21	8.02
CHCl3	11.37	8.87	9.86
Diethyl ether	9.51	9.47	10.54
Tetrahydrofuran	9.38	8.22	9.15
Ethyl acetate	10.01	9.16	10.19
Acetone	9.70	6.37	7.09
Acetonitrile	12.20	4.44	4.94
Toluene	8.83	11.80	13.13
Benzene	9.24	10.35	11.52
Methanol	10.85	3.28	3.65
SiO_2	8.15	5.42	6.04
MgO	7.65	5.47	6.09
ZnO	4.35	5.27	5.86
Zn	9.39	5.82	6.47
Al_2O_3	5.99	5.36	5.96
TiO_2	9.50	7.12	7.92
Carbon	11.26	1.76	1.96

Table 2. Values of the harmonic mean of the ionization energies of SiO_2 particles and organic solvents (in 10^{-19} J) and the parameter $\frac{3\mathcal{N}}{2(4\pi\varepsilon_0)^2}\mathcal{P}_{SiO_2-X}$ (in 10^{-15} SI unit) for the various organic molecules.

Molecule	$\frac{\varepsilon_{SiO_2}\,\varepsilon_X}{(\varepsilon_{SiO_2}+\varepsilon_X)}$ (in 10^{-19}J)	$\frac{3\mathcal{N}}{2(4\pi\varepsilon_0)^2}\mathcal{P}_{SiO_2-X}$ (in 10^{-15} SI)
n-pentane	7.274	58.992
n-hexane	7.226	69.814
n-heptane	7.162	79.135
n-octane	7.119	91.901
n-nonane	7.089	99.919
n-decane	7.069	109.623
CCl_4	7.623	67.151
Nitromethane	7.513	44.956
CH_2Cl_2	7.582	44.379

Preprints (www.preprints.org) | NOT PEER-REVIEWED | Posted: 8 January 2024 doi:10.20944/preprints202401.0638.v1

CHCl3	7.596	54.666
Diethyl ether	7.022	53.988
Tetrahydrofuran	6.977	46.564
Ethyl acetate	7.188	53.453
Acetone	7.087	36.652
Acetonitrile	7.818	28.180
Toluene	6.780	64.955
Benzene	6.930	58.231
Methanol	7.447	19.829

Table 3. Values of the harmonic mean of the ionization energies of MgO particles and organic solvents (in 10^{-19} J) and the parameter $\frac{3\mathcal{N}}{2(4\pi\varepsilon_0)^2}\mathcal{P}_{MgO-X}$ (in 10^{-15} SI unit) for the various organic molecules.

	$\frac{\varepsilon_{MgO}\,\varepsilon_X}{(\varepsilon_{MgO}+\varepsilon_X)}$	$\frac{3\mathcal{N}}{2(4\pi\varepsilon_0)^2}\mathcal{P}_{MgO-X}$
Molecule	**(in 10^{-19}J)**	**(in 10^{-15} SI)**
n-pentane	7.018	56.917
n-hexane	6.974	67.374
n-heptane	6.914	76.393
n-octane	6.874	88.735
n-nonane	6.846	96.490
n-decane	6.828	105.872
CCl_4	7.343	64.680
Nitromethane	7.241	43.325
CH_2Cl_2	7.304	42.754
CHCl3	7.317	52.662
Diethyl ether	6.783	52.153
Tetrahydrofuran	6.742	44.991
Ethyl acetate	6.938	51.595
Acetone	6.844	35.395
Acetonitrile	7.523	27.117
Toluene	6.557	62.820
Benzene	6.697	56.277
Methanol	7.179	19.116

Table 4. Values of the harmonic mean of the ionization energies of ZnO particles and organic solvents (in 10^{-19} J) and the parameter $\frac{3\mathcal{N}}{2(4\pi\varepsilon_0)^2}\mathcal{P}_{ZnO-X}$ (in 10^{-15} SI unit) for the various organic molecules.

	$\frac{\varepsilon_{ZnO}\,\varepsilon_X}{(\varepsilon_{ZnO}+\varepsilon_X)}$	$\frac{3\mathcal{N}}{2(4\pi\varepsilon_0)^2}\mathcal{P}_{ZnO-X}$
Molecule	**(in 10^{-19}J)**	**(in 10^{-15} SI)**
n-pentane	4.891	39.665
n-hexane	4.869	47.041

Preprints (www.preprints.org) | NOT PEER-REVIEWED | Posted: 8 January 2024 doi:10.20944/preprints202401.0638.v1

n-heptane	4.840	53.478
n-octane	4.820	62.224
n-nonane	4.807	67.745
n-decane	4.797	74.392
CCl_4	5.046	44.451
Nitromethane	4.998	29.904
CH_2Cl_2	5.028	29.431
CHCl3	5.034	36.231
Diethyl ether	4.776	36.716
Tetrahydrofuran	4.755	31.732
Ethyl acetate	4.852	36.080
Acetone	4.806	24.852
Acetonitrile	5.131	18.494
Toluene	4.662	44.666
Benzene	4.733	39.769
Methanol	4.968	13.230

Table 5. Values of the harmonic mean of the ionization energies of Monogal-Zn and organic solvents (in 10^{-19} J) and the parameter $\frac{3\mathcal{N}}{2(4\pi\varepsilon_0)^2}\mathcal{P}_{Zn-X}$ (in 10^{-15} SI unit) for the various organic molecules.

	$\frac{\varepsilon_{Zn}\,\varepsilon_X}{(\varepsilon_{Zn}+\varepsilon_X)}$	$\frac{3\mathcal{N}}{2(4\pi\varepsilon_0)^2}\mathcal{P}_{Zn-X}$
Molecule	**(in 10^{-19}J)**	**(in 10^{-15} SI)**
n-pentane	7.852	63.683
n-hexane	7.797	75.326
n-heptane	7.722	85.324
n-octane	7.672	99.042
n-nonane	7.638	107.648
n-decane	7.615	118.076
CCl_4	8.261	72.769
Nitromethane	8.132	48.658
CH_2Cl_2	8.212	48.070
CHCl3	8.228	59.222
Diethyl ether	7.560	58.122
Tetrahydrofuran	7.508	50.105
Ethyl acetate	7.752	57.650
Acetone	7.635	39.486
Acetonitrile	8.490	30.603
Toluene	7.280	69.743
Benzene	7.453	62.627
Methanol	8.054	21.447

Table 6. Values of the harmonic mean of the ionization energies of Al_2O_3 and organic solvents (in 10^{-19} J) and the parameter $\frac{3\mathcal{N}}{2(4\pi\varepsilon_0)^2}\mathcal{P}_{Al_2O_3-X}$ (in 10^{-15} SI unit) for the various organic molecules.

Preprints (www.preprints.org) | NOT PEER-REVIEWED | Posted: 8 January 2024 doi:10.20944/preprints202401.0638.v1

Molecule	$\frac{\varepsilon_{Al_2O_3}\,\varepsilon_X}{(\varepsilon_{Al_2O_3}+\varepsilon_X)}$ (in 10^{-19}J)	$\frac{3\mathcal{N}}{2(4\pi\varepsilon_0)^2}\mathcal{P}_{Al_2O_3-X}$ (in 10^{-15} SI)
n-pentane	6.056	49.114
n-hexane	6.023	58.186
n-heptane	5.978	66.053
n-octane	5.948	76.784
n-nonane	5.927	83.541
n-decane	5.913	91.697
CCl_4	6.296	55.460
Nitromethane	6.221	37.222
CH_2Cl_2	6.268	36.687
CHCl3	6.277	45.177
Diethyl ether	5.880	45.209
Tetrahydrofuran	5.849	39.033
Ethyl acetate	5.996	44.590
Acetone	5.926	30.646
Acetonitrile	6.428	23.171
Toluene	5.710	54.699
Benzene	5.816	48.867
Methanol	6.175	16.443

Table 7. Values of the harmonic mean of the ionization energies of TiO_2 and organic solvents (in 10^{-19} J) and the parameter $\frac{3\mathcal{N}}{2(4\pi\varepsilon_0)^2}\mathcal{P}_{TiO_2-X}$ (in 10^{-15} SI unit) for the various organic molecules.

Molecule	$\frac{\varepsilon_{TiO_2}\,\varepsilon_X}{(\varepsilon_{TiO_2}+\varepsilon_X)}$ (in 10^{-19}J)	$\frac{3\mathcal{N}}{2(4\pi\varepsilon_0)^2}\mathcal{P}_{TiO_2-X}$ (in 10^{-15} SI)
n-pentane	7.900	64.071
n-hexane	7.844	75.781
n-heptane	7.768	85.834
n-octane	7.718	99.631
n-nonane	7.683	108.285
n-decane	7.660	118.773
CCl_4	8.314	73.236
Nitromethane	8.183	48.965
CH_2Cl_2	8.264	48.376
CHCl3	8.281	59.600
Diethyl ether	7.604	58.462
Tetrahydrofuran	7.552	50.396
Ethyl acetate	7.799	57.996
Acetone	7.680	39.719
Acetonitrile	8.546	30.804

Preprints (www.preprints.org) | NOT PEER-REVIEWED | Posted: 8 January 2024 doi:10.20944/preprints202401.0638.v1

Toluene	7.321	70.137
Benzene	7.496	62.988
Methanol	8.104	21.581

Table 8. Values of the harmonic mean of the ionization energies of carbon fibers and organic solvents (in 10^{-19} J) and the parameter $\frac{3\mathcal{N}}{2(4\pi\varepsilon_0)^2}\mathcal{P}_{Carbon-X}$ (in 10^{-15} SI unit) for the various organic molecules.

	$\frac{\varepsilon_{Carbon}\,\varepsilon_X}{(\varepsilon_{Carbon}+\varepsilon_X)}$	$\frac{3\mathcal{N}}{2(4\pi\varepsilon_0)^2}\mathcal{P}_{Carbon-X}$
Molecule	**(in 10^{-19}J)**	**(in 10^{-15} SI)**
n-pentane	8.598	69.736
n-hexane	8.532	82.430
n-heptane	8.443	93.286
n-octane	8.384	108.220
n-nonane	8.342	117.574
n-decane	8.314	128.928
CCl_4	9.091	80.082
Nitromethane	8.935	53.465
CH_2Cl_2	9.032	52.869
CHCl3	9.052	65.147
Diethyl ether	8.249	63.421
Tetrahydrofuran	8.188	54.640
Ethyl acetate	8.479	63.053
Acetone	8.339	43.125
Acetonitrile	9.369	33.772
Toluene	7.917	75.847
Benzene	8.122	68.249
Methanol	8.841	23.543

In this new approach, one gave more precise values of the parameters of molecules such as the deformation polarizability and the harmonic mean of the ionization energies of solids and organic solvents in contrary of those proposed by Donnet et al. [5] that only took the characteristic electronic frequencies of the probes independently of those of the solid. Indeed, Table 2 to 8 clearly showed that the harmonic mean of the ionization energies of the solvents varied as a function of the used solid material.

To show the difference between our values and those of Donnet et al. [5], one presented on Table 9 the values of the deformation polarizability of some polar molecules and two n-alkanes.

Table 9. Values of deformation polarizability (in 10^{-40} C m²/V) compared to those proposed by Donnet et al. of the various organic molecules, with the calculated relative error.

	α_{0X} or α_{0S} (in 10^{-40} C m²/V) (Donnet values)	α_{0X} or α_{0S} (in 10^{-40} C m²/V) (Our values)	Relative error (in %)
Molecule			
n-nonane	19.75	19.32	2.2
n-decane	-	21.25	-

Preprints (www.preprints.org) | NOT PEER-REVIEWED | Posted: 8 January 2024 doi:10.20944/preprints202401.0638.v1

CCl_4	11.68	12.07	3.2
CH_2Cl_2	-	8.02	-
CHCl3	10.57	9.86	7.2
Diethyl ether	9.71	10.54	8.0
Tetrahydrofuran	8.77	9.15	4.2
Ethyl acetate	10.79	10.19	5.9
Acetone	7.12	7.09	0.4
Acetonitrile	5.43	4.94	10.0
Toluene	13.68	13.13	4.2
Benzene	11.95	11.52	3.7
Methanol	-	3.65	-
SiO_2	-	6.04	-
MgO	-	6.09	-
ZnO	-	5.86	-
Zn	-	6.47	-
Al_2O_3	-	5.96	-
TiO_2	-	7.92	-
Carbon	-	1.96	-

Table 9 showed that the values relative to some solvents such as n-decane, dichloromethane and methanol and those of solid particles are not given by Donnet et al. The relative error reaches 10% that can have negative effect on the determination of the specific free energy.

Now, if one adds the error committed by Donnet et al. [5] when neglecting the variations of the harmonic mean of ionization energies $\frac{\varepsilon_S \varepsilon_X}{(\varepsilon_S + \varepsilon_X)}$ for the various polar molecules that vary from 20% to 70%. Indeed, this parameter varies from a solid surface to another solid material. The variation in the value of $\frac{\varepsilon_S \varepsilon_X}{(\varepsilon_S + \varepsilon_X)}$ of organic molecules between two solids can reach 70% in certain cases such as ZnO and TiO_2 (Tables 4 and 7).

4.2. London dispersive surface energy of solid particles by using thermal model

The thermal model [10-14] was used to determine the London dispersive surface energy $\gamma_s^d\ (T)$ of the various solid materials used in this study. This model took into consideration the effect of the temperature on the surface area of organic molecules. The obtained results are presented on Table 10 at several temperatures.

Table 10. Values of the London dispersive surface energy $\gamma_s^d\ (T)$ (in mJ/m²) of the various solid materials

Temperature T(K)	323.15	343.15	363.15	383.15	Equation of $\gamma_s^d\ (T)$
Oxidized carbon fibers	51.59	43.42	35.25	27.08	$\gamma_s^d\ (T)$= -0.408 T + 183.6
Untreated carbon fibers	52.96	47.06	41.16	35.27	$\gamma_s^d\ (T)$= -0.295 T + 148.2
MgO	54.35	47.92	41.71	35.71	$\gamma_s^d\ (T)$= -0.311 T + 154.6
MgO	58.37	53.12	47.87	42.62	$\gamma_s^d\ (T)$= -0.262 T + 143.2
ZnO	59.25	55.07	50.12	44.16	$\gamma_s^d\ (T)$= -0.251 T + 140.8
Al_2O_3	60.98	51.03	41.08	31.13	$\gamma_s^d\ (T)$= -0.497 T + 221.7
Monogal-Zn	81.90	68.84	52.26	37.03	$\gamma_s^d\ (T)$= -0.756 T + 327.0
SiO_2	85.34	67.75	52.86	39.23	$\gamma_s^d\ (T)$= -0.766 T + 331.8

Preprints (www.preprints.org) | NOT PEER-REVIEWED | Posted: 8 January 2024 doi:10.20944/preprints202401.0638.v1

Table 10 showed that the various solid surfaces can be classified with increasing order of their London dispersive surface energy as following:

Oxidized carbon fibers < Untreated carbon fibers < MgO < ZnO < Al_2O_3 < Monogal-Zn < SiO_2

The highest London dispersive surface energy was obtained by the silica particles. One also observed that the dispersive surface energy of the two carbon fibers are very close, and silica and monogal surfaces exhibited close values of γ_s^d. Furthermore, the linearity of $\gamma_s^d\ (T)$ was assured for all materials with an excellent linear regression coefficients approaching 1.000 (Figure 2).

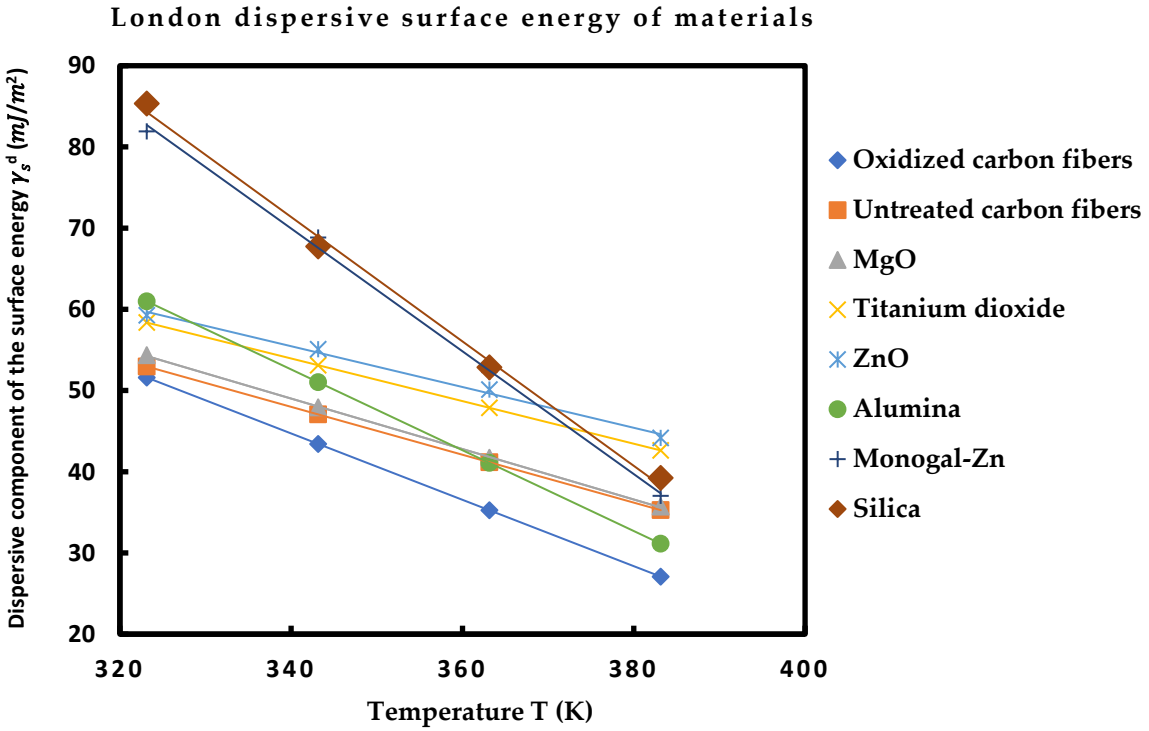

Figure 2. Dispersive component of the surface energy $\gamma_s^d\ (mJ/m^2)$ of solid materials as a function of the temperature T (K).

4.3. Polar surface interactions between solid materials and organic molecules

By using our new method and new findings presented in section 3, one determined the values of the polar free surface energy $(-\Delta G_a^{sp}(T))$ of the various polar solvents adsorbed on the various solid particles as a function of the temperature T. The results were given on Table 11.

Table 11. Values of $(-\Delta G_a^{sp}(T))$ (in kJ/mol) of the various polar molecules adsorbed on the different used solid materials

	Silica			
T(K)	323.15	343.15	363.15	383.15
CCl_4	6.752	6.810	6.881	6.968
Nitromethane	13.573	12.367	11.273	10.191
CH_2Cl_2	22.490	21.846	21.269	20.716
$CHCl_3$	19.752	19.304	18.925	18.546
Diethyl ether	26.838	25.462	23.802	22.314
THF	35.506	32.787	30.435	27.908
Ethyl Acetate	4.566	4.015	3.530	3.079
Acetone	10.612	9.608	8.703	7.816

Preprints (www.preprints.org) | NOT PEER-REVIEWED | Posted: 8 January 2024 doi:10.20944/preprints202401.0638.v1

Acetonitrile	16.734	15.304	14.016	12.738
Toluene	17.330	16.724	16.168	15.598
Benzene	5.640	5.170	4.745	4.328
MgO				
T(K)	323.1500	343.1500	363.1500	383.15
CH_2Cl_2	3.3120	3.7860	4.5320	5.211
$CHCl_3$	5.833	2.693	1.560	2.176
Diethyl ether	14.415	16.559	18.671	20.721
THF	23.053	25.004	26.928	28.797
Acetone	15.723	20.520	25.354	30.243
Ethyl acetate	6.224	7.620	9.112	10.523
ZnO				
T(K)	323.15	343.15	363.15	383.15
CH_2Cl_2	2.4490	1.9151	1.2231	0.6320
$CHCl_3$	1.1506	1.0611	0.9988	0.9325
Diethyl ether	7.7211	7.0452	6.5940	6.0373
THF	13.5961	12.9006	12.2948	11.5175
Ethyl acetate	3.9554	2.7149	1.8004	1.0420
Benzene	0.8696	0.6900	0.5367	0.3535
Monogal-Zn				
T(K)	323.15	343.15	363.15	383.15
CH_2Cl_2	2.354	1.965	1.426	0.854
$CHCl_3$	15.001	11.698	7.938	6.927
Diethyl ether	17.481	15.950	14.408	12.982
THF	23.786	21.503	19.298	17.285
Acetone	22.779	20.603	18.500	16.582
Ethyl acetate	12.287	9.154	5.642	4.895
Alumina				
T(K)	323.15	343.15	363.15	383.15
CCl_4	0.334	0.163	0.084	-
CH_2Cl_2	6.751	6.654	6.575	6.648
$CHCl_3$	38.808	36.648	34.670	32.613
Ether	18.559	16.226	14.028	12.322
THF	41.085	39.144	37.268	35.790
Ethyl acetate	11.624	9.452	7.875	6.125
Toluene	40.532	38.377	36.371	34.878
TiO2				
T(K)	313.15	333.15	353.15	373.15
CH_2Cl_2	2.546	1.924	1.254	0.723
$CHCl_3$	3.146	2.019	0.893	-
THF	7.620	6.620	5.620	4.620
Ethyl Acetate	3.979	2.417	0.857	-

Preprints (www.preprints.org) | NOT PEER-REVIEWED | Posted: 8 January 2024 doi:10.20944/preprints202401.0638.v1

Acetone	5.776	4.068	2.362	0.651
Benzene	5.564	4.199	2.834	1.463
Nitromethane	10.394	9.024	7.657	6.283
Acetonitrile	4.615	2.524	0.433	-1.661
Untreated Carbon fibers				
T(K)	323.15	343.15	363.15	383.15
CCl_4	1.723	1.956	2.203	2.518
CH_2Cl_2	4.096	3.645	3.129	2.548
$CHCl_3$	14.829	13.537	11.761	8.193
Ether	2.112	1.633	1.131	0.546
THF	11.852	11.079	10.310	9.748
C6H6	8.577	8.315	8.055	8.011
Ethyl acetate	9.500	9.251	9.019	8.975
Acetone	10.723	10.282	9.865	9.647
Oxidized Carbon fibers				
T(K)	323.15	343.15	363.15	383.15
CCl_4	2.785	2.843	2.911	2.974
CH_2Cl_2	10.546	9.952	9.379	8.800
$CHCl_3$	12.788	12.228	11.685	11.134
Ether	7.399	6.965	6.548	6.124
THF	17.020	15.878	14.753	13.623
C6H6	10.429	9.943	9.473	8.995
Ethyl acetate	13.212	12.718	12.242	11.758
Acetone	17.928	16.999	16.094	15.183

Table 11 clearly showed the amphoteric behavior of the various solid surfaces with different acid-base interactions depending on the number of the surface group sites present on the solid particles. Table 11 led to classify the polar solvents, for each solid surface in increasing order of the polar free surface energy of interaction.

In the case of silica particles, one obtained the following order:

Ethyl Acetate < CCl4 < Acetone < Nitromethane< Toluene < $CHCl_3$ < CH_2Cl_2 < Diethyl ether < THF

Proving a strong interaction with the acidic organic molecules and lower for the basic solvents and therefore concluding to more basic behavior.

In this case of MgO, the obtained order was:

CH_2Cl_2 < $CHCl_3$< Ethyl acetate < Diethyl ether < Acetone < Tetrahydrofuran

That showed a behvior rather amphoteric.

For ZnO, one also observed a strong amphoteric character:

Benzene < $CHCl_3$ < CH_2Cl_2 < Ethyl acetate < Diethyl ether < Tetrahydrofuran

The amphoteric character was proved for monogal-Zn particles:

CH_2Cl_2 < Ethyl acetate < $CHCl_3$< Diethyl ether < Acetone < Tetrahydrofuran

For alumina, one obtained the following order:

CCl4 < CH_2Cl_2 < Ethyl acetate < Diethyl ether < $CHCl_3$ < Toluene < Tetrahydrofuran

In case of TiO_2:

CH_2Cl_2 < $CHCl_3$< Ethyl acetate < Acetonitrile < Benzene < Acetone < THF < nitromethane

For untreated carbon fibers:

CCl4 < Diethyl ether < CH_2Cl_2 < Benzene < Ethyl acetate < Tetrahydrofuran

Preprints (www.preprints.org) | NOT PEER-REVIEWED | Posted: 8 January 2024 doi:10.20944/preprints202401.0638.v1

and the oxidized carbon fibers presented an amphoteric character:

CCl4 < Diethyl ether < Benzene < CH_2Cl_2 < $CHCl_3$ < Benzene < Ethyl acetate < THF< Acetone

In order to compare the behavior of the various solids as a function of the different polar solvents, one plotted on Figures 3 the variations of $(-\Delta G_a^{sp}(T))$ of the various polar molecules as a function of the temperature.

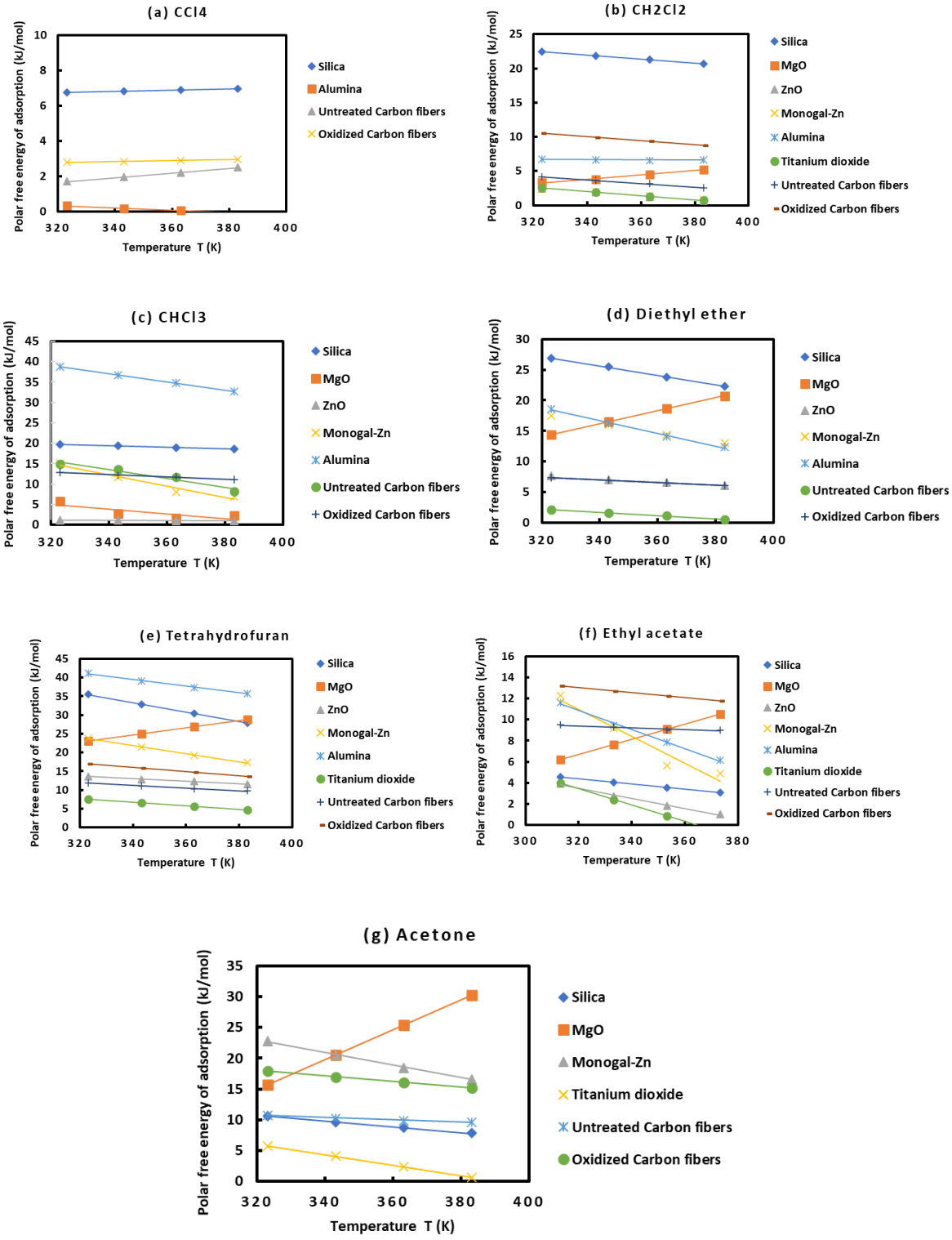

Figure 3. Evolution of the specific free surface energy $(-\Delta G_a^{sp}(T))$ of the various solid materials in interactions with the different polar molecules Such as CCl_4 (a), CH_2Cl_2 (b), $CHCl_3$ (c), diethyl ether (d), tetrahydrofuran (e), ethyl acetate (f), and acetone (g) as function of the temperature.

Preprints (www.preprints.org) | NOT PEER-REVIEWED | Posted: 8 January 2024 doi:10.20944/preprints202401.0638.v1

The results on Figures 3 showed different behaviors of the various solid surfaces in interaction with the polar molecules. One gave the classification of these solid materials in increasing order of their polar free energies with the different polar solvents:

- with CCl4: alumina < untreated carbon fibers < oxidized carbon fibers < silica
- with CH_2Cl_2, Monogal-Zn < ZnO < TiO_2 < MgO < untreated carbon fibers < alumina < oxidized carbon fibers < silica
- with $CHCl_3$, ZnO < MgO < oxidized carbon fibers < untreated carbon fibers < Monogal-Zn < silica < alumina
- with diethyl ether, untreated carbon fibers < oxidized carbon fibers < ZnO < MgO < Monogal-Zn < alumina < silica
- with tetrahydrofuran, TiO_2 < untreated carbon fibers < ZnO < oxidized carbon fibers < MgO < Monogal-Zn < silica < alumina
- with ethyl acetate, TiO_2 < ZnO < silica < MgO < untreated carbon fibers < alumina < monogal-Zn < oxidized carbon fibers
- with acetone, TiO_2 < silica < untreated carbon fibers < MgO < oxidized carbon fibers

These results proved that alumina, silica and oxidized carbon fibers exhibited stronger interactions with the acidic and basic molecules then showing their higher amphoteric character than the other solid substrates.

4.4. Lewis's ethalpic and entropic acid base parameters

By using the results of $\Delta G_a^{sp}(T)$ given on Table 11 and Figures 3, one determined from equation (11), the different values of the polar enthalpy $(-\Delta H_a^{sp})$ and entropy $(-\Delta S_a^{sp})$ of adsorption of the various polar molecules on the solid surfaces. The results were presented on Table 12.

Table 12. Values of polar enthalpy $(-\Delta H_a^{sp}\ in\ kJ\ mol^{-1})$ and entropy $(-\Delta S_a^{sp} in\ J\ K^{-1} mol^{-1})$ of the various polar solvents adsorbed on the various solid surfaces by using our new method.

	Silica	
Polar solvent	$(-\Delta S_a^{sp} in\ J\ K^{-1} mol^{-1})$	$(-\Delta H_a^{sp}\ in\ kJ\ mol^{-1})$
CCl_4	-4.6	5.2514
Nitromethane	52.8	30.543
CH_2Cl_2	27.7	31.377
$CHCl_3$	18.8	25.788
Diethyl ether	77.4	51.914
THF	123.5	75.304
Ethyl acetate	23	11.944
Acetone	43.6	24.624
Acetonitrile	62.2	36.719
Toluene	27.1	26.027
Benzene	20.4	12.173
	MgO	
CH_2Cl_2	32.2	7.1665
$CHCl_3$	-60.5	-24.435
Diethyl ether	105.1	19.543
Ethyl acetate	71.9	17.038
THF	95.8	7.8791

Preprints (www.preprints.org) | NOT PEER-REVIEWED | Posted: 8 January 2024 doi:10.20944/preprints202401.0638.v1

Acetone	242	62.489
Acetonitrile	81.6	2.0138
Toluene	-13.8	15.211
ZnO		
CH_2Cl_2	20.9	8.9949
$CHCl_3$	-11.4	1.0743
Diethyl ether	18.5	18.218
THF	23.8	26.647
Ethyl acetate	38.2	17.176
Benzene	-1.0	6.7082
Monogal		
CH_2Cl_2	25.2	10.547
$CHCl_3$	139.9	59.803
Diethyl ether	75.2	41.760
THF	108.5	58.796
Ethyl acetate	44.2	21.674
Acetone	103.5	56.155
Acetonitrile	110.8	54.921
Toluene	99.9	54.474
Alumina		
CCl_4	6.2	2.314
CH_2Cl_2	1.9	7.3421
$CHCl_3$	102.8	71.989
Diethyl ether	104.6	52.207
THF	88.8	69.683
Ethyl acetate	90.4	40.683
Toluene	94.9	71.036
Titanium dioxide		
CH_2Cl_2	30.7	12.146
$CHCl_3$	56.4	20.818
THF	10.0	23.277
Ethyl Acetate	78.1	28.448
Acetone	85.4	32.518
Benzene	68.3	26.965
Nitromethane	68.5	31.846
Acetonitrile	104.6	37.370
Untreated carbon fibers		
CCl_4	-13.2	-2.4181
CH_2Cl_2	25.8	12.209
$CHCl_3$	108.4	49.284
Benzene	9.8	11.602
Diethyl ether	26	10.275

Preprints (www.preprints.org) | NOT PEER-REVIEWED | Posted: 8 January 2024 doi:10.20944/preprints202401.0638.v1

THF	35.4	22.895
Ethyl acetate	9	12.289
Acetone	18.2	16.380
Oxidized carbon fibers		
CCl_4	3.2	1.7876
CH_2Cl_2	29.1	19.639
$CHCl_3$	27.5	21.406
Benzene	23.9	17.897
Diethyl ether	21.2	14.038
THF	56.6	34.733
Ethyl acetate	24.2	20.782
Acetone	45.7	32.230

Table 12 also showed a difference in the behavior of the various solid surfaces in interaction with acidic, basic and amphoteric polar solvents. In order to qunatify the acid-base constants of the solid materials, one used equations (13) and (23). The obtained values of Lewis enthalpic acid base constants K_A and K_D and Lewis entropic acid base constants ω_A and ω_D of the different solid particles were presented on Table 13. The comparison of the acid-base behavior of the different solid materials allowed to classify them in decreasing order of acidity and basicity.

For the acidity, one obtained the following classification:

Silica > alumina > Monogal-Zn > TiO_2 > ZnO > oxidized carbon fibers > untreated carbon fibers > MgO

Whereas, the comparison between their basicity led to give the following order:

Oxidized carbon fibers > alumina > untreated carbon fibers > ZnO > Monogal-Zn > Silica > MgO > TiO_2

By comparing the various solids in decreasing order of their ratio K_D/K_A, on found the following classification:

Oxidized carbon fibers > untreated carbon fibers > MgO > ZnO > TiO_2 > alumina > Monogal-Zn > Silica

The last classification seems to be very interesting, because the oxidization of carbon fibers will increase the polar surface groups and therefore their basicity, in contrary to the behavior of silica that exhibits higher acidity than the other solid surfaces.

Table 13. Values of the enthalpic acid base constants K_A and K_D (unitless) and the entropic acid base constants ω_A and ω_D (unitless) of the various solid surfaces and the corresponding acid base ratios.

Solid surfaces	K_A	K_D	K_D/K_A	R^2	$10^3.\omega_A$	$10^3.\omega_D$	ω_D / ω_A	R^2
Silica	0.73	1.45	2.0	0.6509	1.23	1.45	1.2	0.651
MgO	0.08	1.13	14.0	0.1722	1.16	0.57	0.5	0.8126
ZnO	0.22	1.63	7.4	0.422	0.29	0.08	0.3	0.8761
Monogal-Zn	0.59	1.49	2.5	0.7296	1.07	3.08	2.9	0.7295
Alumina	0.71	2.21	3.1	0.7301	0.92	4.21	4.6	0.7739
Titanium dioxide	0.25	0.87	3.5	0.9874	0.86	1.80	2.1	0.9804
Untreated Carbon fibers	0.13	2.19	16.8	0.0799	0.30	1.56	5.2	0.3195
Oxidized Carbon fibers	0.20	3.41	17.4	0.0779	0.37	4.32	11.6	0.141

Preprints (www.preprints.org) | NOT PEER-REVIEWED | Posted: 8 January 2024 doi:10.20944/preprints202401.0638.v1

However, when we observed the linear regression coeffcients given on Table 13, one found that the liearity of equations (13) and (23) are not satisfied for most of the solid surfaces. In such case, a correction has to be executed. To do that, one used equation (17) and resolved the linear system with three unkown numbers. The solution was perofrmed for all solids except for titanium dioxide that presented an excellent linear regression coefficient. The more results were given on Table 14.

Table 14. Corrected values of Lewis's acid-base constants K_A, K_D and K of the various solid surfaces and the corresponding acid base ratios.

Solid surfaces	K_A	K_D	K	K_D/K_A
Silica	1.105	3.572	0.186	3.23
MgO	0.005	0.336	-0.045	71.66
ZnO	0.401	2.418	0.089	6.03
Monogal-Zn	0.782	3.477	0.113	4.45
Alumina	0.988	3.291	0.136	3.33
Untreated Carbon fibers	0.359	3.339	0.110	9.29
Oxidized Carbon fibers	0.529	5.085	0.161	9.61

Table 14 gave the corrected values of the acid-base constants with an additional constant called coupling constant reflecting the amphoteric character of materials.

One obsrved that the classification of acidity of different solid materials was conserved after correction, however it was changed for the basicity. One found the following classification of solid surfaces in decreasing basicity:

Oxidized carbon fibers > silica > monogal-Zn > untreated carbon fibers > alumina > ZnO > TiO_2 > MgO

It was proved that the oxidized carbon fibers exhibited the strongest basicity, whereas, silica had the highest acidity. It was also showed the MgO presented more neutral surface with small basic tendency.

4.5. Consequences of the application of the new method

The first scientific result of the application of the new parameter $\mathcal{P}_{SX} = \frac{\varepsilon_S \varepsilon_X}{(\varepsilon_S + \varepsilon_X)} \alpha_{0X}$ relative to the interaction between solids and organic molecule was the separation between the London dispersive energy and the polar free energy of the adsorption of polar organic molecules and solid surfaces. It is the first time that we were able to calculate exactly the two contributions of the free surface energy of interaction. Equation (6) was perfectly applied for all solids and solvents with an excellent linear regression coefficient approaching 1.000 and the determination of the slope A of the straight line given by equation (6) in the case of n-alkanes adsorbed on solid surfaces conducted to calcule the London dipersive energy of interaction not only for n-alkanes, but also for polar organic solvents by using the following relation

$$\Delta G_a^d(T) = A\left[\frac{3\mathcal{N}}{2(4\pi\varepsilon_0)^2}\mathcal{P}_{SX}\right] \qquad (24)$$

With this new approach, one characterized all studied solids by giving on Tables S1 to S16, the two London dispersive and polar free energies of interaction between solids and organic molecules. This also allowed to obtain the total free surface energy of adsorption without calculating the surface specific area of the considered solid materials.

The second consequence was to clearly verify the insufficiency of the approach proposed by Donnet et al. [5]. Indeed, if we applied their method on silica particles, one obtained the values of $(-\Delta G_a^{sp}(T))$ of polar solvents adsorbed on silica surfaces. These results compared to our new findings were presented on Table 15.

Preprints (www.preprints.org) | NOT PEER-REVIEWED | Posted: 8 January 2024 doi:10.20944/preprints202401.0638.v1

Table 15. Values of $(-\Delta G_a^{sp}(T)\ in\ kJ\ mol^{-1})$, $(-\Delta S_a^{sp} in\ J\ K^{-1} mol^{-1})$ and $(-\Delta H_a^{sp}\ in\ kJ\ mol^{-1})$ of polar molecules adsorbed on silica surfaces by comparing Donnet et al.'s method and our new method .

Results by using Donnet et al.'s method							
T(K)	323.15	343.15	363.15	383.15	403.15	$(-\Delta S_a^{sp} in\ J\ K^{-1} mol^{-1})$	$(-\Delta H_a^{sp}\ in\ kJ\ mol^{-1})$
CCl4	34.616	31.401	28.904	26.818	24.489	124.2	74.643
Nitromethane	34.014	30.151	27.038	24.328	21.424	155	83.687
CH2Cl2	53.122	48.974	45.622	42.692	39.626	166.4	106.43
CHCl3	48.598	44.795	41.775	39.150	36.312	151.1	96.995
Diethyl ether	53.703	49.136	44.982	41.394	37.319	202.5	118.86
THF	57.922	52.382	47.865	43.564	39.053	232.8	132.69
Ethyl Acetate	33.315	29.418	26.298	23.608	20.724	155	82.944
Acetone	25.935	22.701	20.154	18.016	15.527	127.5	66.771
Acetonitrile	25.145	22.059	19.641	17.621	15.228	121.4	64.011
Toluene	55.833	51.069	47.157	43.631	40.161	193.9	117.99
Benzene	38.564	34.399	31.032	28.069	25.006	167.2	92.143
Results by using our new method							
T(K)	323.15	343.15	363.15	383.15	403.15	$(-\Delta S_a^{sp} in\ J\ K^{-1} mol^{-1})$	$(-\Delta H_a^{sp}\ in\ kJ\ mol^{-1})$
CCl4	6.752	6.810	6.881	6.968	7.129	5.2514	6.752
Nitromethane	13.573	12.367	11.273	10.191	9.378	30.543	13.573
CH2Cl2	22.490	21.846	21.269	20.716	20.287	31.377	22.490
CHCl3	19.752	19.304	18.925	18.546	18.250	25.788	19.752
Diethyl ether	26.838	25.462	23.802	22.314	20.676	51.914	26.838
THF	35.506	32.787	30.435	27.908	25.593	75.304	35.506
Ethyl Acetate	4.566	4.015	3.530	3.079	2.732	11.944	4.566
Acetone	10.612	9.608	8.703	7.816	7.144	24.624	10.612
Acetonitrile	16.734	15.304	14.016	12.738	11.793	36.719	16.734
Toluene	17.330	16.724	16.168	15.598	15.187	26.027	17.330
Benzene	5.640	5.170	4.745	4.328	4.026	12.173	5.640

The results on Table 15 clearly showed a large difference between the values obtained by the two above methods. The calculation of the ratios $\frac{(-\Delta G_a^{sp}(Donnet\ et\ al.)}{(-\Delta G_a^{sp}(Hamieh))}$, $\frac{(-\Delta S_a^{sp}(Donnet\ et\ al.)}{(-\Delta S_a^{sp}(Hamieh))}$ and $\frac{(-\Delta H_a^{sp}(Donnet\ et\ al.)}{(-\Delta H_a^{sp}(Hamieh))}$ given on Table 16 showed a surestimation of the values of $(-\Delta G_a^{sp}(T)$ obtained by Donnet et al. method varying from 1.3 to 7.7 times the values obtained by our new method. Whereas, in the calculation of the specific entropy and enthalpy, Table 16 showed ratios varying from 3.1 to 23.7 strongly depending on the adsorbed polar molecule. However, one globaly found a ratio approaching 2 for most of polar molecules.

Table 16. Values of the ratios $\frac{(-\Delta G_a^{sp}(Donnet\ et\ al.)}{(-\Delta G_a^{sp}(Hamieh))}$ at different temperatures, and $\frac{(-\Delta S_a^{sp}(Donnet\ et\ al.)}{(-\Delta S_a^{sp}(Hamieh))}$ and $\frac{(-\Delta H_a^{sp}(Donnet\ et\ al.)}{(-\Delta H_a^{sp}(Hamieh))}$ of the various polar organic molecules

T(K)	323.15	343.15	363.15	383.15	403.15	$(-\Delta S_a^{sp} in\ J\ K^{-1} mol^{-1})$	$(-\Delta H_a^{sp}\ in\ kJ\ mol^{-1})$
CCl4	5.1	4.6	4.2	3.8	3.4	23.7	11.1
Nitromethane	2.5	2.4	2.4	2.4	2.3	5.1	6.2
CH2Cl2	2.4	2.2	2.1	2.1	2.0	5.3	4.7

Preprints (www.preprints.org) | NOT PEER-REVIEWED | Posted: 8 January 2024 doi:10.20944/preprints202401.0638.v1

CHCl3	2.5	2.3	2.2	2.1	2.0	5.9	4.9
Diethyl ether	2.0	1.9	1.9	1.9	1.8	3.9	4.4
THF	1.6	1.6	1.6	1.6	1.5	3.1	3.7
Ethyl Acetate	7.3	7.3	7.5	7.7	7.6	13.0	18.2
Acetone	2.4	2.4	2.3	2.3	2.2	5.2	6.3
Acetonitrile	1.5	1.4	1.4	1.4	1.3	3.3	3.8
Toluene	3.2	3.1	2.9	2.8	2.6	7.4	6.8
Benzene	6.8	6.7	6.5	6.5	6.2	13.7	16.3

These large variations of the values obtained by applying Donnet et al. method is certainly due to the fact that this method omitted the variation of the harmonic mean $\overline{\varepsilon_{S-X}}$ of the ionization energies of the solid and the adsorbed polar solvent given by relation (25).

$$\overline{\varepsilon_{S-X}} = \frac{\varepsilon_S\ \varepsilon_X}{(\varepsilon_S + \varepsilon_X)} \tag{25}$$

Donnet et al. used the concept $\alpha_0\sqrt{\nu_0}$ or $\alpha_{0X}\sqrt{\varepsilon_X}$. The variations of $\overline{\varepsilon_{S-X}}$ is not identical to those of $\sqrt{\varepsilon_X}$ of the interaction solid-polar molecule as it was shown by Table 17.

Table 17. Harmonic mean $\overline{\varepsilon_{S-X}}$ (in 10^{-19}J) values of the ionization energies of the various materials and the adsorbed polar solvents found in our new approach, and values of $\sqrt{\varepsilon_X}$ (in $10^{-10}J^{1/2}$) used by Donnet et al. method.

Molecule	$\overline{\varepsilon_{SiO2-X}}$ (in 10^{-19}J)	$\overline{\varepsilon_{MgO-X}}$ (in 10^{-19}J)	$\overline{\varepsilon_{ZnO-X}}$ (in 10^{-19}J)	$\overline{\varepsilon_{Zn-X}}$ (in 10^{-19}J)	$\overline{\varepsilon_{Al2O3-X}}$ (in 10^{-19}J)	$\overline{\varepsilon_{TiO2-X}}$ (in 10^{-19}J)	$\overline{\varepsilon_{C-X}}$ (in 10^{-19}J)	$\sqrt{\varepsilon_X}$ (in $10^{-10}J^{1/2}$)
n-pentane	7.27	7.02	4.89	7.85	6.06	7.90	8.60	12.83
n-hexane	7.23	6.97	4.87	7.80	6.02	7.84	8.53	12.73
n-heptane	7.16	6.91	4.84	7.72	5.98	7.77	8.44	12.61
n-octane	7.12	6.87	4.82	7.67	5.95	7.72	8.38	12.52
n-nonane	7.09	6.85	4.81	7.64	5.93	7.68	8.34	12.46
n-decane	7.07	6.83	4.80	7.62	5.91	7.66	8.31	12.43
CCl_4	7.62	7.34	5.05	8.26	6.30	8.31	9.09	13.55
Nitromethane	7.51	7.24	5.00	8.13	6.22	8.18	8.94	13.32
CH_2Cl_2	7.58	7.30	5.03	8.21	6.27	8.26	9.03	13.46
CHCl3	7.60	7.32	5.03	8.23	6.28	8.28	9.05	13.49
Diethyl ether	7.02	6.78	4.78	7.56	5.88	7.60	8.25	12.34
Tetrahydrofuran	6.98	6.74	4.76	7.51	5.85	7.55	8.19	12.25
Ethyl acetate	7.19	6.94	4.85	7.75	6.00	7.80	8.48	12.66
Acetone	7.09	6.84	4.81	7.64	5.93	7.68	8.34	12.46
Acetonitrile	7.82	7.52	5.13	8.49	6.43	8.55	8.60	13.97
Toluene	6.78	6.56	4.66	7.28	5.71	7.32	8.53	11.89
Benzene	6.93	7.02	4.73	7.45	5.82	7.50	8.44	12.16
Methanol	7.45	6.97	4.97	8.05	6.18	8.10	8.38	13.18

It was observed on Table 17 that the harmonic mean $\overline{\varepsilon_{S-X}}$ strongly depend on the interaction between the solid and the polar solvent and cannot be considered as constant for all studied materials as was supposed by the method proposed by Donnet et al.

Preprints (www.preprints.org) | NOT PEER-REVIEWED | Posted: 8 January 2024 doi:10.20944/preprints202401.0638.v1

The third consequence of our new approach was the determination of the average separation distance H between the solid particle and the organic moolecule as a function of the temperature when the deformation polarizability of the solid is known. By using equation (7) and the experimental results, one gave on Table 18 the values of the average separation distance H at different temperatures for the various solid substrates.

Table 18. Values of the average separation distance H (in Å) btween the various solid substrates and the organic molecules at different temperatures.

T(K)	323.15	343.15	363.15	383.15
SiO2	5.05	5.12	5.19	5.27
MgO	5.23	5.27	5.31	5.35
ZnO	4.87	4.88	4.89	4.90
Monogal	5.18	5.24	5.33	5.44
Al2O3	5.03	5.08	5.13	5.16
TiO2	5.51	5.53	5.54	5.56
Untreated carbon fibers	4.45	4.48	4.50	4.52
Oxidized carbon fibers	4.49	4.54	4.59	4.64

Table 18 showed that the average separation distance H is comprised between 4.45 Å and 5.56 Å for the various solid particles. A slight increasing effect of the temperature on the separation distance was observed in all studied solid substrates. Furthermore, one observed that the separation distance between a solid and an organic molecule is an intrinsic parameter of the solid. Table 18 allowed to classify the various solid materials in increasing order of the separation distance for all temperatures:

Untreated carbon fibers ≈ Oxidized carbon fibers > ZnO > alumina > Monogal-Zn > Silica > MgO > TiO_2

This classification is very close to that obtained with the basicity of solid materials. It seems that when the basicity or the ratio K_D/K_A decreases, the separation distance slightly increases to reach a maximum value with TiO_2 equal to 5.50 Å.

The fourth consequence of this new method was to be able to give with more accuracy the values of the acid-base surface energy of the various solid materials. Indeed, by applying Van Oss et al. relation [29] that gave the specific enthalpy of adsorption as a function of the Lewis acid surface energy of the solid surface γ_s^+ and the solvent γ_l^+; and the corresponding Lewis base surface energy (γ_s^- for the surface and γ_l^- for the solvent) by equation (26)

$$\Delta G_a^{sp}(T) = 2\mathcal{N}a\left(\sqrt{\gamma_l^-\gamma_s^+} + \sqrt{\gamma_l^+\gamma_s^-}\right) \tag{26}$$

By choosing two monopolar solvents such as ethyl acetate (EA) and dichloromethane characterized by:

$$\begin{cases}\gamma_{CH2Cl2}^+ = 5.2\ mJ/m^2\ , \gamma_{CH2Cl2}^- = 0\\ \gamma_{EA}^+ = 0\ , \qquad \gamma_{EA}^- = 19.2\ mJ/m^2\end{cases} \tag{27}$$

The Lewis's acid and base surface energies of a solid surface $\gamma_s^+$and γ_s^-can be obtained from relations (26) and (27):

$$\begin{cases}\gamma_s^+ = \dfrac{\left[\Delta G_a^{sp}(T)\ (EA)\right]^2}{4\mathcal{N}^2[a(EA)]^2\gamma_{EA}^-}\\ \gamma_s^- = \dfrac{\left[\Delta G_a^{sp}(T)\ (CH2Cl2)\right]^2}{4\mathcal{N}^2[a(CH2Cl2)]^2\gamma_{CH2Cl2}^+}\end{cases} \tag{28}$$

The experimental values of free specific energy of ethyl acetate $\Delta G_a^{sp}(T)\,(EA)$ and dichloromethane $\Delta G_a^{sp}(T)\ (CH2Cl2)$ given in Table 19, one determined the values of the specific acid

Preprints (www.preprints.org) | NOT PEER-REVIEWED | Posted: 8 January 2024 doi:10.20944/preprints202401.0638.v1

and base surface energy contributions γ_s^+, γ_s^- as well as the acid-base surface energy γ_s^{AB} given by relation (29):

$$\gamma_s^{AB} = 2\sqrt{\gamma_s^+ \gamma_s^-} \quad (29)$$

Table 19. Values of $(-\Delta G_a^{sp}(T)\ in\ kJ/mol)$ of the dichloromethane and the ethyl acetate adsorbed on the different solid materials at various temperatures.

$(-\Delta G_a^{sp}(T)\ in\ kJ/mol)$ of dichloromethane				
T(K)	323.15	343.15	363.15	383.15
SiO2	22.49	21.846	21.269	20.716
MgO	3.312	3.786	4.532	5.211
ZnO	2.449	1.9151	1.2231	0.632
Monogal	2.354	1.965	1.426	0.854
Al2O3	6.751	6.654	6.575	6.648
TiO2	2.546	1.924	1.254	0.723
Untreated carbon fibers	4.096	3.645	3.129	2.548
Oxidized carbon fibers	10.546	9.952	9.379	8.8
$(-\Delta G_a^{sp}(T)\ in\ kJ/mol)$ of ethyl acetate				
T(K)	323.15	343.15	363.15	383.15
SiO2	4.566	4.015	3.53	3.079
MgO	6.224	7.62	9.112	10.523
ZnO	3.9554	2.7149	1.8004	1.042
Monogal	12.287	9.154	5.642	4.895
Al2O3	11.624	9.452	7.875	6.125
TiO2	3.979	2.417	0.857	-
Untreated carbon fibers	9.500	9.251	9.019	8.975
Oxidized carbon fibers	13.212	12.718	12.242	11.758

By using the values given on tables 10 and 19, and relation (29), one presented on Table 20 the Lewis's acid and base surface energies of solid particles γ_s^+, γ_s^-, γ_s^{AB} and the total surface energy $\gamma_s^{tot.}$ of the various solid materials. The total surface energy $\gamma_s^{tot.}$ of the solid surfaces was obtained by using relation (30):

$$\gamma_s^{tot.} = \gamma_s^d + \gamma_s^{AB} \quad (30)$$

The values of the dispersive surface energy of the different solid materials were taken from table 10.

Table 20. Values of the specific acid and base surface energy contributions γ_s^+, γ_s^-, γ_s^{AB} and $\gamma_s^{tot.}$ (in mJ/m²) of the different solid surfaces.

Values of γ_s^+ (in mJ/m²)				
T(K)	323.15	343.15	363.15	383.15
SiO_2	8.11	6.15	4.66	3.47
MgO	15.07	22.14	31.03	40.57
ZnO	6.08	2.81	1.21	0.40
Monogal	58.72	31.95	11.90	8.78

Preprints (www.preprints.org) | NOT PEER-REVIEWED | Posted: 8 January 2024 doi:10.20944/preprints202401.0638.v1

Al_2O_3	52.55	34.06	23.18	13.75
TiO_2	6.16	2.23	0.27	0.03
Untreated carbon fibers	33.54	31.08	28.63	26.18
Oxidized carbon fibers	64.04	57.33	50.62	43.91
Values of γ_s^- (in mJ/m²)				
T(K)	323.15	343.15	363.15	383.15
SiO_2	275.18	254.53	236.49	219.94
MgO	5.97	7.64	10.74	13.92
ZnO	3.26	1.96	0.78	0.20
Monogal	3.01	2.06	1.06	0.37
Al_2O_3	24.80	23.61	22.60	22.65
TiO_2	3.53	1.97	0.82	0.27
Untreated carbon fibers	8.01	5.99	3.98	1.96
Oxidized carbon fibers	55.89	48.21	40.53	32.85
Values of γ_s^{AB}(in mJ/m²)				
T(K)	323.15	343.15	363.15	383.15
SiO_2	94.46	79.11	66.37	55.27
MgO	18.96	26.02	36.51	47.52
ZnO	8.91	4.69	1.95	0.57
Monogal	26.61	16.22	7.11	3.62
Al_2O_3	65.95	56.00	46.05	36.11
TiO_2	9.32	4.19	0.95	0.17
Untreated carbon fibers	32.75	27.04	21.32	15.61
Oxidized carbon fibers	119.64	105.11	90.58	76.04
Values of $\gamma_s^{tot.}$(in mJ/m²)				
T(K)	323.15	343.15	363.15	383.15
SiO_2	179.80	146.86	119.23	94.50
MgO	76.31	77.15	81.42	86.23
ZnO	71.12	61.88	54.11	47.71
Monogal	116.87	91.36	67.14	48.53
Al_2O_3	128.31	106.07	86.64	67.71
TiO_2	70.06	60.18	51.74	45.15
Untreated carbon fibers	85.71	74.10	62.49	50.87
Oxidized carbon fibers	171.23	148.53	125.83	103.13

The values of the different acid-base surface energies of the various solid substrates given on Table 20 showed that the oxidized carbon fibers and the silica particles gave the highest values of γ_s^-, γ_s^{AB} and $\gamma_s^{tot.}$ followed by alumina particles and monogal-Zn surfaces, whereas, the oxidized carbon fibers and alumina surfaces gave larger values of γ_s^+ again confirming the highest acid-base properties of these materials. The determination of the ratio γ_s^{AB}/γ_s^d of the solid materials showed that this ratio varies from 12% for ZnO particles to reach 70% for the oxidized carbon fibers and about 50% for silica and alumina surfaces. This clearly proved the strong contribution of acid-base surface energy relative to the corresponding London dispersive energy.

Preprints (www.preprints.org) | NOT PEER-REVIEWED | Posted: 8 January 2024 doi:10.20944/preprints202401.0638.v1

5. Conclusions

A new method of separation of London dispersive and polar surface energy was proposed by using the inverse gas chromatography technique (IGC) at infinite dilution. The parameter of polarizability of organic molecules adsorbed on eight different solid materials was used to propose a new parameter taking into account all terms involved in the expression of London dispersive energy of interaction. The originality of this new method concerned the full determination and use of a new intrinsic thermodynamic parameter $\mathcal{P}_{SX} = \frac{\varepsilon_S \varepsilon_X}{(\varepsilon_S + \varepsilon_X)} \alpha_{0X}$ reflecting the London dispersive energy of interaction between solid materials and organicmolecules. One calculated the parameter $\mathcal{P}_{SX}$ for different materials and organic molecules. Experimental results obtained by IGC allowed to determine the average separation distance solid-organic solvents at different temperatures. The dispersive free energy and the polar energy of n-alkanes and polar probes were determined by this method. The thermal model was used to quantify the London dispersive surface energy $\gamma_s^d(T)$ of the various solid materials at different temperatures and allowed to determine the different components γ_s^+, γ_s^- and γ_s^{AB} of acid-base surface energies of solid particles as well as their total surface energy $\gamma_s^{tot.}$. Results showed the highest acid-base surface energy was obtained by the oxidized carbon fibers followed by silica particles and alumina surfaces.

The determination of the polar interaction energy $\Delta G_a^{sp}(T)$ of the different polar molecules adsorbed on the solid materials allowed to obtain the polar enthalpy and entropy of interaction and therefore the enthalpic and entropic Lewis's acid-base constants. The results showed that all studied solid surfaces exhibited amphoteric behavior with stronger Lewis's basicity. The oxidized and untreated carbon fibers, ZnO and silica particles showed an important basic force, whereas, silica, alumina, monogal-Zn presented the highest Lewis's acidity.

The application of the classic equation (12) allowing the determination of the acid-base constants showed poor linear regression coefficients. It was corrected by using Hamieh model that added a coupling constant reflecting the amphoteric character of solid materials.

It was proved that the method proposed by Donnet et al. neglected the values of harmonic mean $\overline{\varepsilon_{S-X}}$ of ionization energies of solids and solvents and this conducted to a surestimation of the specific or polar free energy of interaction reaching in several cases 5 times the corrected value. By taking into account the different values of harmonic mean and the deformation polarizability of n-alkanes and polar organic molecules, one obtained more accurate values of the London dispersive energy, the polar energy, the acid-base constants and the acid-base surface energies of the various solids in interaction with several polar molecules.

Supplementary Materials: The following supporting information can be downloaded at: www.mdpi.com/xxx/s1, **Table S1.** Values (in kJ/mol) of London dispersive energy ($-\Delta G_a^d(T)$) of n-alkanes and polar solvents adsorbed on silica particles at different temperatures. **Table S2.** Values (in kJ/mol) of London dispersive energy ($-\Delta G_a^{sp}(T)$) of polar solvents adsorbed on silica particles at different temperatures. **Table S3.** Values (in kJ/mol) of London dispersive energy ($-\Delta G_a^d(T)$) of n-alkanes and polar solvents adsorbed on MgO particles at different temperatures. **Table S4.** Values (in kJ/mol) of London dispersive energy ($-\Delta G_a^{sp}(T)$) of polar solvents adsorbed on MgO particles at different temperatures. **Table S5.** Values (in kJ/mol) of London dispersive energy ($-\Delta G_a^d(T)$) of n-alkanes and polar solvents adsorbed on ZnO particles at different temperatures. **Table S6.** Values (in kJ/mol) of London dispersive energy ($-\Delta G_a^{sp}(T)$) of polar solvents adsorbed on ZnO particles at different temperatures. **Table S7.** Values (in kJ/mol) of London dispersive energy ($-\Delta G_a^d(T)$) of n-alkanes and polar solvents adsorbed on monogal-Zn particles at different temperatures. **Table S8.** Values (in kJ/mol) of London dispersive energy ($-\Delta G_a^{sp}(T)$) of polar solvents adsorbed on monogal-Zn particles at different temperatures. **Table S9.** Values (in kJ/mol) of London dispersive energy ($-\Delta G_a^d(T)$) of n-alkanes and polar solvents adsorbed on alumina particles at different temperatures. **Table S10.** Values (in kJ/mol) of London dispersive energy ($-\Delta G_a^{sp}(T)$) of polar solvents adsorbed on alumina particles at different temperatures. **Table S11.** Values (in kJ/mol) of London dispersive energy ($-\Delta G_a^d(T)$) of n-alkanes and polar solvents adsorbed on TiO_2 particles at different temperatures. **Table S12.** Values (in kJ/mol) of London dispersive energy ($-\Delta G_a^{sp}(T)$) of polar solvents adsorbed on TiO_2 particles at different temperatures. **Table S13.** Values (in kJ/mol) of London dispersive energy ($-\Delta G_a^d(T)$) of n-alkanes and polar solvents adsorbed on untreated carbon fibers particles at different temperatures. **Table S14.** Values (in kJ/mol) of London dispersive energy ($-\Delta G_a^{sp}(T)$) of polar solvents adsorbed on untreated carbon fibers particles at different temperatures. **Table S15.** Values (in kJ/mol) of London

dispersive energy ($-\Delta G_a^d(T)$) of n-alkanes and polar solvents adsorbed on oxidized carbon fibers at different temperatures. **Table S16.** Values (in kJ/mol) of London dispersive energy ($-\Delta G_a^{sp}(T)$) of polar solvents adsorbed on oxidized carbon fibers at different temperatures.

Conflicts of Interest: "The author declares no conflict of interest."

References

1. C. Saint-Flour, E. Papirer, Gas-solid chromatography. A method of measuring surface free energy characteristics of short carbon fibers. 1. Through adsorption isotherms, Ind. Eng. Chem. Prod. Res. Dev., 21 (1982) 337-341, doi: 10.1021/i300006a029.
2. C. Saint-Flour, E. Papirer, Gas-solid chromatography: method of measuring surface free energy characteristics of short fibers. 2. Through retention volumes measured near zero surface coverage, Ind. Eng. Chem. Prod. Res. Dev., 21 (1982) 666-669, doi: 10.1021/i300008a031.
3. C. Saint-Flour and E. Papirer, "Gas-solid chromatography: a quick method of estimating surface free energy variations induced by the treatment of short glass fibers." *Journal of Colloid and Interface Science* 91 (1983): 69-75.
4. J. Schultz, L. Lavielle, C. Martin, The role of the interface in carbon fibre-epoxy composites. J. Adhes., 23 (1987) 45–60
5. J.-B. Donnet, S. Park, H. Balard, Evaluation of specific interactions of solid surfaces by inverse gas chromatography, Chromatographia, 31 (1991) 434–440.
6. E. Brendlé, E. Papirer, A new topological index for molecular probes used in inverse gas chromatography for the surface nanorugosity evaluation, 2. Application for the Evaluation of the Solid Surface Specific Interaction Potential, J. Colloid Interface Sci., 194 (1997) 217–2224.
7. E. Brendlé, E. Papirer, A new topological index for molecular probes used in inverse gas chromatography for the surface nanorugosity evaluation, 1. Method of Evaluation, J. Colloid Interface Sci., 194 (1997) 207–216.
8. D.T. Sawyer, D.J. Brookman. Thermodynamically based gas chromatographic retention index for organic molecules using salt-modified aluminas and porous silica beads, *Anal. Chem*. 1968, 40, 1847-1850. https://doi.org/10.1021/ac60268a015.
9. M.M. Chehimi, E. Pigois-Landureau, Determination of acid–base properties of solid materials by inverse gas chromatography at infinite dilution. A novel empirical method based on the dispersive contribution to the heat of vaporization of probes, J. Mater. Chem., 4 (1994) 741–745.
10. T Hamieh, Study of the temperature effect on the surface area of model organic molecules, the dispersive surface energy and the surface properties of solids by inverse gas chromatography, *J. Chromatogr. A*, 1627 (2020) 461372.
11. T Hamieh, AA Ahmad, T Roques-Carmes, J Toufaily, New approach to determine the surface and interface thermodynamic properties of H-β-zeolite/rhodium catalysts by inverse gas chromatography at infinite dilution, Scientific Reports, 10 (1) (2020) 1-27.
12. T Hamieh, New methodology to study the dispersive component of the surface energy and acid–base properties of silica particles by inverse gas chromatography at infinite dilution, Journal of Chromatographic Science 60 (2) (2022) 126-142, https://doi.org/10.1093/chromsci/bmab066
13. T. Hamieh, New Physicochemical Methodology for the Determination of the Surface Thermodynamic Properties of Solid Particles. *AppliedChem* 2023, *3*(2), 229-255; https://doi.org/10.3390/appliedchem3020015.
14. Hamieh, T.; Schultz J. Study of the adsorption of n-alkanes on polyethylene surface - State equations, molecule areas and covered surface fraction, *Comptes Rendus de l'Académie des Sciences, Série IIb* **1996,** 323 (4), 281-289,
15. *F. London*, The general theory of molecular forces, Trans. Faraday. Soc.,**33**, (1937), pp. 8-26.
16. Conder, J.R.; Locke, D.C.; Purnell, J.H. Concurrent solution and adsorption phenomena in chromatography. *I. J. Phys. Chem.* **1969,** 73, 700-8. https://doi.org/10.1021/j100723a035.
17. Conder, J.R.; Purnell, J.H. Gas chromatography at finite concentrations. Part 2.—A generalized retention theory. *Trans Faraday Soc.* **1968,** 64, 3100–11.
18. Conder, J.R.; Purnell, J.H. Gas chromatography at finite concentrations. Part 3.—Theory of frontal and elution techniques of thermodynamic measurement. *Trans Faraday Soc.* **1969,** 65, 824-38. https://doi.org/10.1039/TF9696500824
19. Conder, J.R.; Purnell, J.H. Gas chromatography at finite concentrations. Part 4.—Experimental evaluation ofmethods for thermodynamic study of solutions. *Trans Faraday Soc.* **1969,** 65, 839-48. https://doi.org/10.1039/TF9696500839
20. Conder, J.R.; Purnell, J.H. Gas chromatography at finite concentrations. Part 1.—Effect of gas imperfection on calculation of the activity coefficient in solution from experimental data. *Trans Faraday Soc.* **1968,** 64, 1505-12. https://doi.org/10.1039/TF9686401505.

21. Vidal, A.; Papirer, E.; Jiao, W.M.; Donnet, J.B. Modification of silica surfaces by grafting of alkyl chains. I-Characterization of silica surfaces by inverse gas–solid chromatography at zero surface coverage. *Chromatographia* **1987,** 23, 121-8. https://doi.org/10.1007/BF02312887
22. Papirer, E.; Balard, H.; Vidal, A. Inverse gas chromatography: a valuable method for the surface characterization of fillers for polymers (glass fibres and silicas). *Eur Polym J.* **1988**, 24, 783-90. https://doi.org/10.1016/0014-3057(88)90015-8
23. Voelkel, A. Inverse gas chromatography: characterization of polymers, fibers, modified silicas, and surfactants. *Crit Rev Anal Chem.* **1991**, 22, 411-39. https://doi.org/10.1080/10408349108051641.
24. Guillet, J. E.; Romansky, M.; Price, G.J.; Van der Mark, R. Studies of polymer structure and interactions by automated inverse gas chromatography. Inverse gas chromatography. 1989, Washington, DC: Characterization of Polymers and Other Materials, American Chemical Society 20–32. *Eng. Asp.*, **2002,** 206, 547-554.
25. V. Gutmann, The Donor-acceptor Approach to Molecular Interactions, Plenum. New York, 1978.
26. Riddle, F. L.; Fowkes, F. M. Spectral shifts in acid-base chemistry. Van der Waals contributions to acceptor numbers, Spectral shifts in acid-base chemistry. 1. van der Waals contributions to acceptor numbers. **1990**, *J. Am. Chem. Soc.*, 112 (9), 3259-3264. https://doi.org/10.1021/ja00165a001.
27. T. Hamieh, M. Rageul-Lescouet, M. Nardin, H. Haidara et J. Schultz, Study of acid-base interactions between some metallic oxides and model organic molecules", *Colloids and Surfaces A: Physicochemical and Engineering Aspects*, 125, 1997, 155-161.
28. David R. Lide, ed., CRC Handbook of Chemistry and Physics, Internet Version 2007, (87th Edition), <http:/www.hbcpnetbase.com>, Taylor and Francis, Boca Raton, FL, 2007.
29. C.J. Van Oss, R.J. Good, M.K. Chaudhury, Additive and nonadditive surface tension components and the interpretation of contact angles, Langmuir, 1988, 4 (4) 884, http:// dx.doi.org/10.1021/la00082a018.